Lab on a Chip

PAPER

View Article Online
View Journal | View Issue

Cite this: *Lab Chip*, 2018, **18**, 323

High-throughput double emulsion-based microfluidic production of hydrogel microspheres with tunable chemical functionalities toward biomolecular conjugation†

Eric Y. Liu,[a] Sukwon Jung,[a] David A. Weitz,[b] Hyunmin Yi*[a] and Chang-Hyung Choi*[c]

Chemically functional hydrogel microspheres hold significant potential in a range of applications including biosensing, drug delivery, and tissue engineering due to their high degree of flexibility in imparting a range of functions. In this work, we present a simple, efficient, and high-throughput capillary microfluidic approach for controlled fabrication of monodisperse and chemically functional hydrogel microspheres *via* formation of double emulsion drops with an ultra-thin oil shell as a sacrificial template. This method utilizes spontaneous dewetting of the oil phase upon polymerization and transfer into aqueous solution, resulting in poly(ethylene glycol) (PEG)-based microspheres containing primary amines (chitosan, CS) or carboxylates (acrylic acid, AA) for chemical functionality. Simple fluorescent labelling of the as-prepared microspheres shows the presence of abundant, uniformly distributed and readily tunable functional groups throughout the microspheres. Furthermore, we show the utility of chitosan's primary amine as an efficient conjugation handle at physiological pH due to its low pKa by direct comparison with other primary amines. We also report the utility of these microspheres in biomolecular conjugation using model fluorescent proteins, R-phycoerythrin (R-PE) and green fluorescent protein (GFPuv), *via* tetrazine–*trans*-cyclooctene (Tz–TCO) ligation for CS-PEG microspheres and carbodiimide chemistry for AA-PEG microspheres, respectively. The results show rapid coupling of R-PE with the microspheres' functional groups with minimal non-specific adsorption. In-depth protein conjugation kinetics studies with our microspheres highlight the differences in reaction and diffusion of R-PE with CS-PEG and AA-PEG microspheres. Finally, we demonstrate orthogonal one-pot protein conjugation of R-PE and GFPuv with CS-PEG and AA-PEG microspheres *via* simple size-based encoding. Combined, these results represent a significant advancement in the rapid and reliable fabrication of monodisperse and chemically functional hydrogel microspheres with tunable properties.

Received 10th October 2017,
Accepted 6th December 2017

DOI: 10.1039/c7lc01088e

rsc.li/loc

Introduction

Hydrogel microparticles hold significant potential in a broad range of applications including biosensing,[1,2] drug delivery[3,4] and tissue engineering.[5,6] This potential is gaining more traction from recent advances in materials and fabrication methods that have enabled the reliable production of microparticles with controlled properties including shape, size, chemical function, and porosity.[7,8] For example, batch processing-based photolithographic[9,10] and micromolding techniques[11–13] allow for reliable fabrication of chemically functional microparticles with precise control over particle shape and dimensions. Meanwhile, microfluidic techniques allow for the high-throughput fabrication of microparticles with readily tunable size and complex geometries.[14] Precise control over microfluidic flows and inclusion of micro-RNA's,[15] cells[16] or other functional components in prepolymer solutions have enabled the development of high throughput fabrication techniques for multiplexed microparticle arrays for biosensing or tissue engineering applications.

However, there still exist critical challenges and gaps in developing these potent microparticle systems despite recent advancements. Notably, while there are numerous reports of uniform microparticles imparted with magnetic, biodegradable, encoding, or DNA-, drug- or cell-carrying function,[14]

[a] *Department of Chemical and Biological Engineering, Tufts University, Medford, Massachusetts, 02155, USA. E-mail: hyunmin.yi@tufts.edu*
[b] *John A. Paulson School of Engineering and Applied Sciences, Harvard University, Cambridge, Massachusetts, 02138, USA*
[c] *Division of Cosmetic Science and Technology, Daegu Haany University, Gyeongsan, 38610, Republic of Korea. E-mail: cchoi@dhu.ac.kr*

† Electronic supplementary information (ESI) available: Raw epifluorescence micrographs of protein-conjugated chitosan microspheres in Fig. 6; negative controls for one pot assembly in Fig. 7. See DOI: 10.1039/c7lc01088e

there has been a lack of reports of such microparticles with uniform chemical functionality.[17] In addition, while providing reliable routes to uniform and chemically functional hydrogel microspheres, the batch-based nature of micromolding techniques limits throughput.[18] The incorporation of tunable and uniform chemical functionalities into hydrogel microparticles in a rapid, high-throughput microfluidic fabrication method would thus represent a significant step forward, for example by enabling facile post-fabrication biofunctionalization with molecular probes.

Our approach to addressing these challenges is an integrated fabrication–conjugation scheme utilizing a rapid microfluidic fabrication of chemically functional hydrogel microspheres, followed by efficient chemical reactions for biomolecular conjugation. In this report, we first demonstrate fabrication of poly(ethylene glycol) (PEG)-based hydrogel microspheres with two potent chemically functional groups, namely primary amines from an aminopolysaccharide chitosan (CS) and carboxylates from acrylic acid (AA), *via* a capillary microfluidic setup based on a novel sacrificial double emulsion-based approach (Fig. 1a). Unlike conventional microfluidics-based methods, this microfluidic setup produces double emulsion drops with an ultra-thin oil shell as templates, leading to reliable manufacturing of highly monodisperse hydrogel particles with minimal use of oil phase and without harsh washing steps. Simple fluorescent labelling reactions show that the primary amines of CS are efficient toward amine-reactive chemistries near physiological pH conditions due to its low p*K*a[19] value by direct comparison with amines with typical p*K*a values found in biomolecules. Next, we utilize a bright red fluorescent protein R-phycoerythrin (R-PE) as a model protein to demonstrate biomolecular conjugation *via* a rapid and high yield bioorthogonal reaction as well as the commonly enlisted carbodiimide chemistry, and utilize these schemes to thoroughly examine and compare the bioconjugation kinetics and polymer network structures of CS-PEG and AA-PEG microspheres. Finally, we show the potential for one-pot biomolecular assembly using the two mutually orthogonal reactions with simple size-based encoding. Combined, we believe that the results in this report illustrate a significant step forward for programmable high-throughput fabrication and biomolecular conjugation approaches that can be readily expanded to overcome limitations in a range of application areas including rapid biosensing, medical diagnostics and biological threat detection in suspension array formats requiring minimal sample volume.

Results and discussion

Rapid capillary microfluidic fabrication of functional hydrogel microspheres

We first demonstrate a potent and high-throughput capillary microfluidic-based fabrication of hydrogel microspheres using a sacrificial double emulsion-based approach, as shown in Fig. 1a. The capillary device consists of three circular capillaries with different tapered orifice sizes inserted into a square capillary.[20] The injection and collection capillaries are chemically treated to impart hydrophobic and hydrophilic surface properties, respectively. Thus, the oil and the aqueous phases preferably wet and can flow smoothly through each capillary. Both capillaries are precisely aligned and closely positioned with the distal end of the collection capillary sealed to the square capillary. In addition, a small tapered circular capillary is inserted into the injection capillary to supply the polymerizable aqueous phase. Finally, the collection capillary is connected to a polyethylene microtubing where ultraviolet (UV) light-induced free radical polymerization occurs before the polymerized hydrogel microspheres are collected in a container (Experimental).

The coaxial biphasic flow in the confined injection capillary results in a thin oil layer fully surrounding the

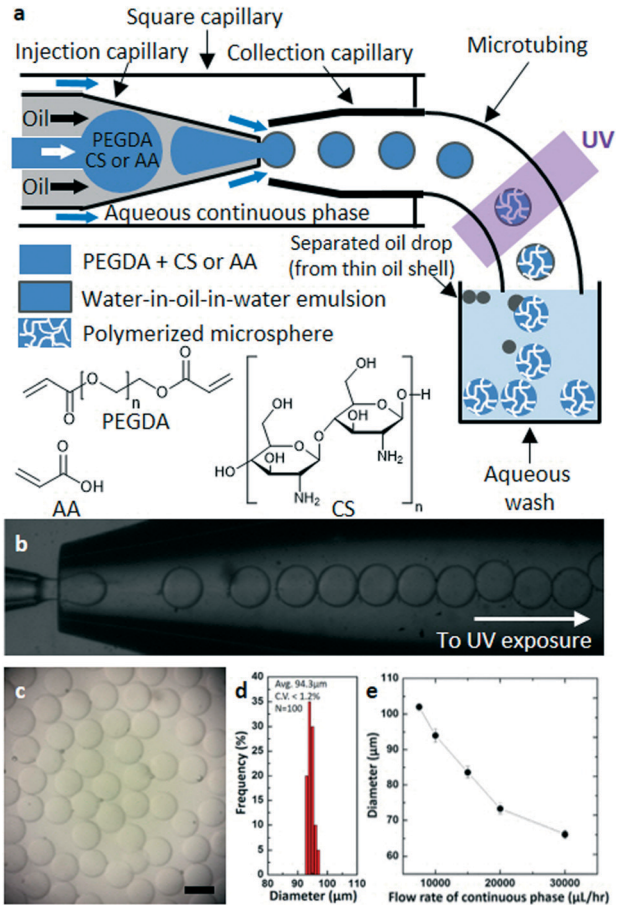

Fig. 1 One-step capillary microfluidic fabrication of chemically functional PEG microspheres *via* double emulsion drops with ultra-thin oil layer. (a) Schematic diagram of the glass capillary microfluidic device used to prepare double emulsion drops containing PEGDA, photoinitiator, inert PEG600 porogen and either CS or AA in the inner-most drop. These drops are polymerized *via* UV light-induced free radical polymerization and collected in an aqueous wash to dewet the oil layer from the polymerized microspheres. (b) Brightfield micrograph of the formation of double emulsion drops. (c) Brightfield micrograph of microspheres with uniform size. Scale bar represents 100 μm. (d) Size distribution of microspheres. (e) Plot of microsphere diameter *vs.* flow rate of the continuous phase showing control over microsphere size.

polymerizable fluid due to strong affinity of the oil phase to the hydrophobic inner wall of the injection capillary. An additional aqueous continuous phase is injected through the interstices between the square and the circular injection capillaries from the same side of the injection capillary, while the interstices of the square and circular collection capillaries at the distal end are sealed, preventing leakage flow and thus making strong shear force toward the collection capillary. The coaxial flow from the injection capillary is emulsified by the continuous aqueous phase near the injection capillary's exit, resulting in monodisperse double emulsion drops with the ultra-thin oil layer flowing through the collection capillary. These drops are then exposed to UV irradiation (estimated exposure time: 5 s) in the end of polyethylene tubing (10 cm) that is connected with the collection capillary (5 cm), forming crosslinked polymeric hydrogel microspheres coated with the oil shell in a continuous manner without any blockage in the injection capillary from undesired UV exposure to the polymerizable fluid. When these as-formed drops are dispersed in the collection container containing deionized (DI) water, the oil shells start to dewet from the surfaces of the drops, leaving hydrogel microspheres,[16] while the separated oil drops immediately migrate to the top due to buoyancy ($\rho_{\text{hexadecane}}$ = 0.770 g mL^{-1} and $\rho_{10\%\ \text{PEGDA aq.}}$ = 1.01 g mL^{-1}).

As shown in the photomicrograph of Fig. 1b, this simple yet potent setup yields exceedingly uniform poly(ethylene glycol) (PEG) hydrogel microspheres in a high throughput manner (*i.e.*, approximately 400 spheres per s) as further illustrated in the brightfield micrograph of Fig. 1c. Detailed size analysis of a representative batch of the as-prepared microspheres in Fig. 1d shows coefficient variation of less than 1.2%, clearly indicating the uniformity of the microspheres and robustness of the microfluidic setup. Furthermore, the size of the microspheres is readily controlled by tuning simple parameters; for example, Fig. 1e shows that one can create microspheres with highly uniform diameters in 65–103 μm ranges simply by changing the flow rate of the aqueous continuous phase (5–30 mL h^{-1}).

Compared to conventional single emulsion (*i.e.* water-in-oil emulsion) based approaches,[21,22] this approach enables production of hydrogel microspheres without any extra washing or separation procedure due to the aqueous continuous flow and spontaneous dewetting of the sacrificial oil layer.[16,23] This thus eliminates the use of large amounts of immiscible oil phase as the carrier fluid, making the process simple and cost-efficient.[16] In short summary, the results in Fig. 1 demonstrate a facile high-throughput fabrication technique for readily controllable manufacturing of hydrogel microspheres.

Chemical functionality of chitosan-poly(ethylene glycol) (CS-PEG) microspheres

Next, we use fluorescent labelling to demonstrate the chemical functionality and uniform incorporation of chitosan in the PEG (CS-PEG) microspheres, as shown in Fig. 2. For this,

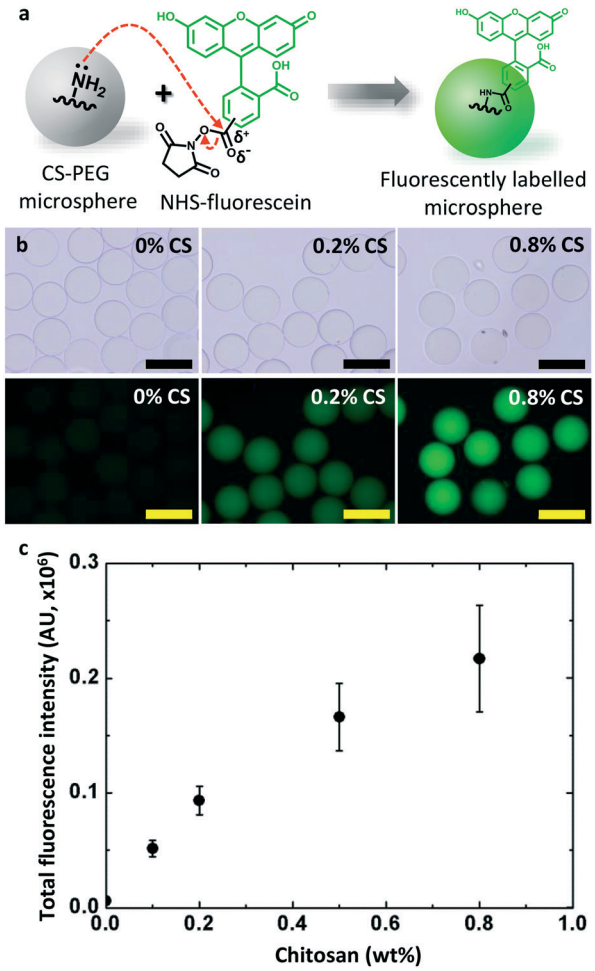

Fig. 2 Fluorescent labelling with CS-PEG microspheres. (a) Schematic diagram of NHS-fluorescein labelling with CS-PEG microspheres. (b) Brightfield (top row) and epifluorescence (bottom row) micrographs of fluorescently labelled CS-PEG microspheres prepared with 0–0.8 wt% CS. Scale bars represent 200 μm. (c) Plot of total fluorescence intensity *vs.* wt% chitosan in the prepolymer solution showing consistent incorporation of chitosan in the microspheres.

we fabricated CS-PEG microspheres by including short chain chitosan (Mn 5 kDa) in the PEGDA prepolymer mixture. The as-prepared CS-PEG microspheres were exposed to an *N*-hydroxysuccinimidyl (NHS) ester form of fluorescein, as shown in the schematic diagram of Fig. 2a. The unshared pair of electrons from CS's amine attacks the electron-deficient carbonyl group of the NHS-fluorescein, leading to the formation of stable amide bond (*i.e.* amidation) in an acyl substitution reaction.[24] This simple reaction thus is a useful tool to examine the presence, chemical functionality and spatial distribution of CS in CS-PEG microspheres.

First, the brightfield micrographs in the first row of Fig. 2b show consistently uniform sizes of the CS-PEG microspheres with varying CS contents upon reaction with NHS-fluorescein, consistent with the results in Fig. 1. Next, the epifluorescence (top view) micrographs in the second row of Fig. 2b show minimal fluorescence for microspheres prepared without CS and increasingly bright and uniform

fluorescence for those prepared with increasing CS content from 0.2–0.8%, indicating that there is minimal non-specific adsorption of fluorescein and that CS is consistently retained within the microspheres. The fluorescence among microspheres in each condition appears uniform, further indicating reliable fabrication of the microspheres and consistent incorporation of CS. Moreover, the fluorescence within each microsphere appears uniform for each condition, suggesting uniform distribution of CS throughout each microsphere. Due to its small size (M.W. 473.4 Da), NHS-fluorescein rapidly penetrates through the polymer networks and reacts with the available primary amine moieties of CS, which are presumably incorporated with the polymer networks *via* Michael addition in a stable manner.[25] This result thus clearly illustrates the chemical functionality and uniform incorporation of CS in the microspheres.

We then quantified the total fluorescence for CS-PEG microspheres prepared with varying CS contents, as shown in Fig. 2c. For this, we used ImageJ software to measure the average fluorescence intensity of a sphere multiplied by its associated area to generate a total fluorescence intensity value, averaged over at least 10–20 spheres per condition examined. The total fluorescence intensity plot of Fig. 2c shows strong positive correlation with higher CS content in the prepolymer solution. This result indicates that CS is consistently incorporated in the microspheres, consistent with our recent studies on micromolding-based CS-PEG microparticles.[24,26]

In short summary, the simple fluorescein labelling results in Fig. 2 illustrate abundant primary amine functionality and consistent, uniform incorporation of CS in CS-PEG microspheres fabricated *via* our rapid capillary microfluidic process.

Chemical functionality of acrylic acid-poly(ethylene glycol) (AA-PEG) microspheres

We next demonstrate carboxylate functionality and uniform incorporation of acrylic acid (AA) in AA-PEG microspheres *via* fluorescent labelling with EDC/NHS chemistry, as shown in Fig. 3. For this, we fabricated AA-PEG microspheres under identical fabrication conditions as the CS-PEG microspheres (Fig. 2), replacing CS with 0–0.5 vol% AA in the prepolymer mixture. We then exposed the as-prepared AA-PEG microspheres to a 4 to 1 mixture of 1-ethyl-3-(3-dimethylaminopropyl)carbodiimide (EDC) and *N*-hydroxysuccimidic acid (NHS), which converts the carboxylates in the AA-PEG microspheres into NHS esters[27] as shown in the schematic diagram of Fig. 3a. These NHS ester-activated microspheres were then reacted with a primary amine-containing dye fluorescein glycine amide (FGA) *via* acyl substitution reaction. Similar to the NHS-fluorescein reaction with the CS-PEG microspheres shown in Fig. 2 yet in reverse direction (*i.e.* amine group on the fluorescent marker instead of CS), this widely used reaction scheme is thus useful in examining the presence and chemical functionality of the carboxyl groups in microspheres.

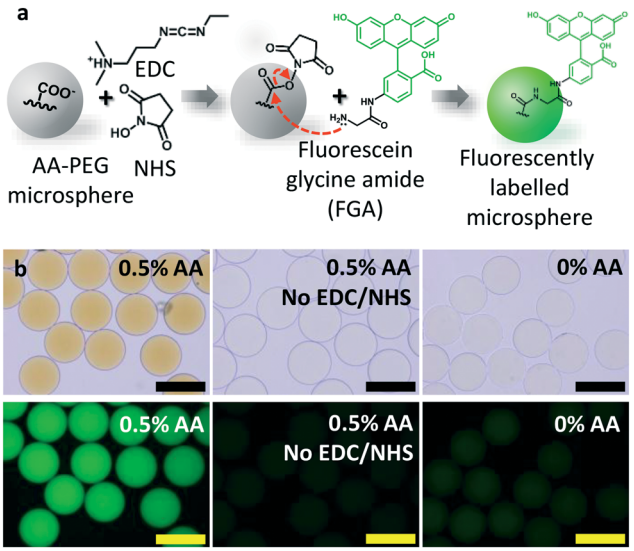

Fig. 3 Fluorescent labelling with AA-PEG microspheres. (a) Schematic diagram of the EDC/NHS activation followed by FGA labelling with AA-PEG microspheres. (b) Brightfield (top row) and epifluorescence (bottom row) micrographs of FGA labelling and negative controls. Scale bars represent 200 μm.

First as shown in the brightfield micrographs in the top row of Fig. 3b, the FGA-labelled AA-PEG microspheres are highly uniform in size, again indicating the robust nature of the capillary microfluidic process. Of note, the AA-PEG microspheres display intense yellow colour upon fluorescent labelling *via* EDC/NHS reaction, suggesting abundant carboxylate functionality. Next, the epifluorescence micrographs (top view) in the bottom row of Fig. 3b show bright and uniform fluorescence among and within AA-PEG microspheres, indicating that AA-PEG microspheres contain abundant and uniformly incorporated carboxylates. Meanwhile, AA-PEG microspheres without NHS ester activation and microspheres without AA show minimal fluorescence upon identical EDC/NHS and FGA exposure (middle and rightmost images at the bottom row of Fig. 3b respectively). These two results indicate that EDC/NHS is required for the conversion of carboxylates into NHS esters for the covalent coupling with the primary amine of FGA, and that there exists minimal non-specific adsorption of FGA with the PEG microspheres, consistent with our recent report on micromolding-based microspheres.[18] In summary, the simple fluorescein labelling results in Fig. 3 clearly illustrate the abundant carboxylate functionality and uniform incorporation of AA in the AA-PEG microspheres.

Effect of pH: CS as an efficient conjugation handle

Upon examining the chemical functionality of our CS-PEG and AA-PEG microspheres, we next studied the effect of pH in the NHS ester–amine reaction on the microspheres' conjugation efficiency. Briefly, we hypothesized that CS is a substantially more efficient conjugation handle at lower and/or physiological pH due to the difference in p*K*a of chitosan's primary amines (6.4[19]) with other primary amines (*i.e.*, FGA's

p*K*a 8.2[28]). For this, we carried out the fluorescent labelling reactions described in the previous results (Fig. 2 and 3) at varying pH (6–9) conditions. As shown in the epifluorescence micrographs in the top row of Fig. 4a, CS-PEG microspheres labelled with excess NHS-fluorescein display uniform and increasingly bright fluorescence with increasing pH.

Similarly, in the bottom row of Fig. 4a, NHS ester-activated AA-PEG microspheres labelled with the identical excess concentration of FGA also display uniform and increasingly bright fluorescence with increasing pH. These trends reflect the increasing nucleophilic character with increasing pH of the primary amines within the CS-PEG microspheres or FGA, thereby increasing the reaction rate relative to that of hydrolysis,[29] and thus increasing the fluorescence intensity of the microspheres.

The normalized fluorescence intensity measurements in Fig. 4b provide further semi-quantitative comparison of this observation. Here, the fluorescence intensity of CS-PEG microspheres significantly increases from pH 6–7, reaching 70% maximum value at pH 7 and 80% at pH 8, while the fluorescence intensity of AA-PEG microspheres reaches only 40% of maximum value at pH 7 and 70% at pH 8. This clear difference in the conjugation efficiency at neutral pH (black arrows) arises from the uniquely low p*K*a (6.4)[19] of chitosan's primary amine compared to that of FGA (p*K*a 8.2).[28] That is, a significant portion of primary amines in CS are deprotonated at pH 7 compared to those of FGA, resulting in higher fluorescence in CS-PEG microspheres. At pH 8, a significant portion of the primary amines of the FGA molecules become deprotonated, yielding higher fluorescence intensity of the AA-PEG microspheres. This result highlights the efficiency of chitosan's primary amines as conjugation handles at lower pH compared to those of primary amines commonly present in biomacromolecules such as from N-termini (p*K*a 7.7) and lysines (p*K*a 10.5) of proteins.[30]

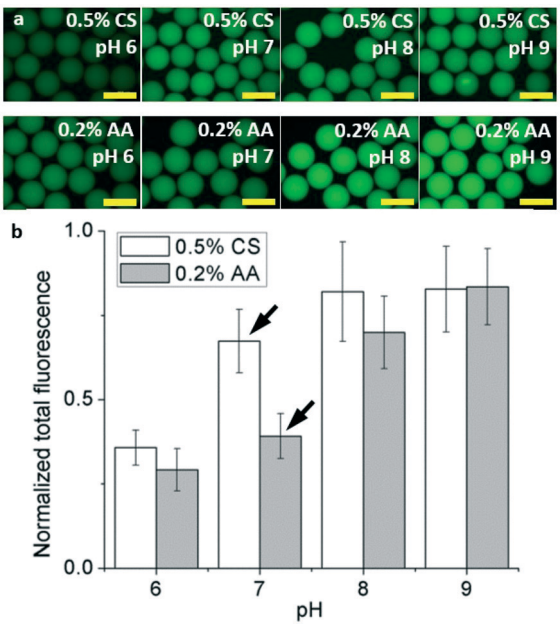

Fig. 4 Comparison of fluorescent labelling with CS-PEG and AA-PEG microspheres at pH 6–9. (a) Epifluorescence micrographs of fluorescently labelled CS-PEG (top row) and AA-PEG (bottom row) microspheres at pH 6–9. Scale bars represent 200 μm. (b) Plot of normalized total fluorescence intensity *vs.* pH for CS-PEG and AA-PEG microspheres.

Selective protein conjugation with CS-PEG and AA-PEG microspheres

To investigate the utility of the microspheres for biofunctionalization, we next examined protein conjugation with CS-PEG and AA-PEG microspheres using a large fluorescent model protein R-phycoerythrin (R-PE) *via* two conjugation reaction schemes. For the CS-PEG microspheres, we utilized biorthogonal tetrazine–*trans*-cyclooctene (Tz–TCO) chemistry[31,32] to covalently couple the primary amines of the microspheres with those of the R-PEs.

For this, we separately activated the primary amines in CS-PEG microspheres with Tz-PEG$_5$-NHS ester and the primary amines on R-PE with TCO-PEG$_4$-NHS ester respectively, as shown in the schematic diagram of Fig. 5a. These Tz-activated CS-PEG microspheres were then exposed to the TCO-modified R-PE and imaged *via* epifluorescence

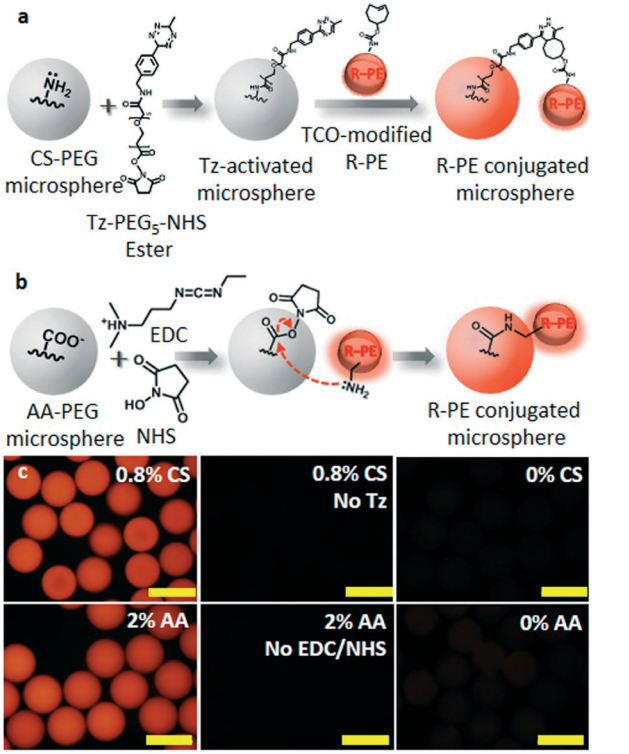

Fig. 5 R-PE conjugation with CS-PEG and AA-PEG microspheres. (a) Schematic of Tz–TCO reaction for R-PE conjugation with CS-PEG microspheres. (b) Schematic of EDC/NHS reaction for R-PE conjugation with AA-PEG microspheres. (c) Epifluorescence micrographs of R-PE conjugation with CS-PEG (top row) and AA-PEG (bottom row) microspheres and negative controls. Scale bars represent 200 μm.

microscopy. For AA-PEG microspheres, we utilized the EDC/NHS chemistry (Fig. 5b) to covalently couple the carboxylates in the microspheres with the primary amines of the R-PEs. For both reaction schemes, we performed the conjugation reactions for 8 h and at fixed R-PE concentration (2 μM).

As shown in the epifluorescence micrographs in the first column of Fig. 5c, both types of microspheres fluoresce brightly and uniformly among microspheres upon R-PE conjugation, indicating that both types can readily be coupled with large proteins (*i.e.* 240 kDa, 11 nm D_H).[33] In addition, the uniformly high fluorescence within each microsphere suggests that proteins have penetrated throughout the polymer networks of the respective type of microspheres, suggesting large hydrogel mesh size. The fluorescence of the CS-PEG microspheres results from the inverse electron demand Diels–Alder reaction between the Tz from the Tz-activated microspheres and the TCO on the TCO-modified R-PEs,[31,32] while the fluorescence of the AA-PEG microspheres results from the acyl substitution of NHS ester-activated AA-PEG microspheres with the primary amines on R-PE.[27,29] In direct contrast, microspheres show minimal fluorescence when reacted in the presence of R-PE either without prior microsphere activation with Tz or requisite functional groups (second and third columns of Fig. 5c). These results indicate that both CS-PEG and AA-PEG microspheres have minimal non-specific adsorption with R-PE, presumably due to the non-fouling nature of the PEG, CS and AA.[34,35] In turn, the minimal fluorescence of these negative controls indicate that the fluorescence observed in the first column of Fig. 5c is primarily due to the covalent coupling of R-PE with the functional groups in CS-PEG and AA-PEG microspheres. The results in Fig. 5 thus demonstrate the utility of CS-PEG and AA-PEG microspheres in selective conjugation of large proteins *via* two conjugation reaction schemes, while suggesting macroporous nature of the polymer networks.

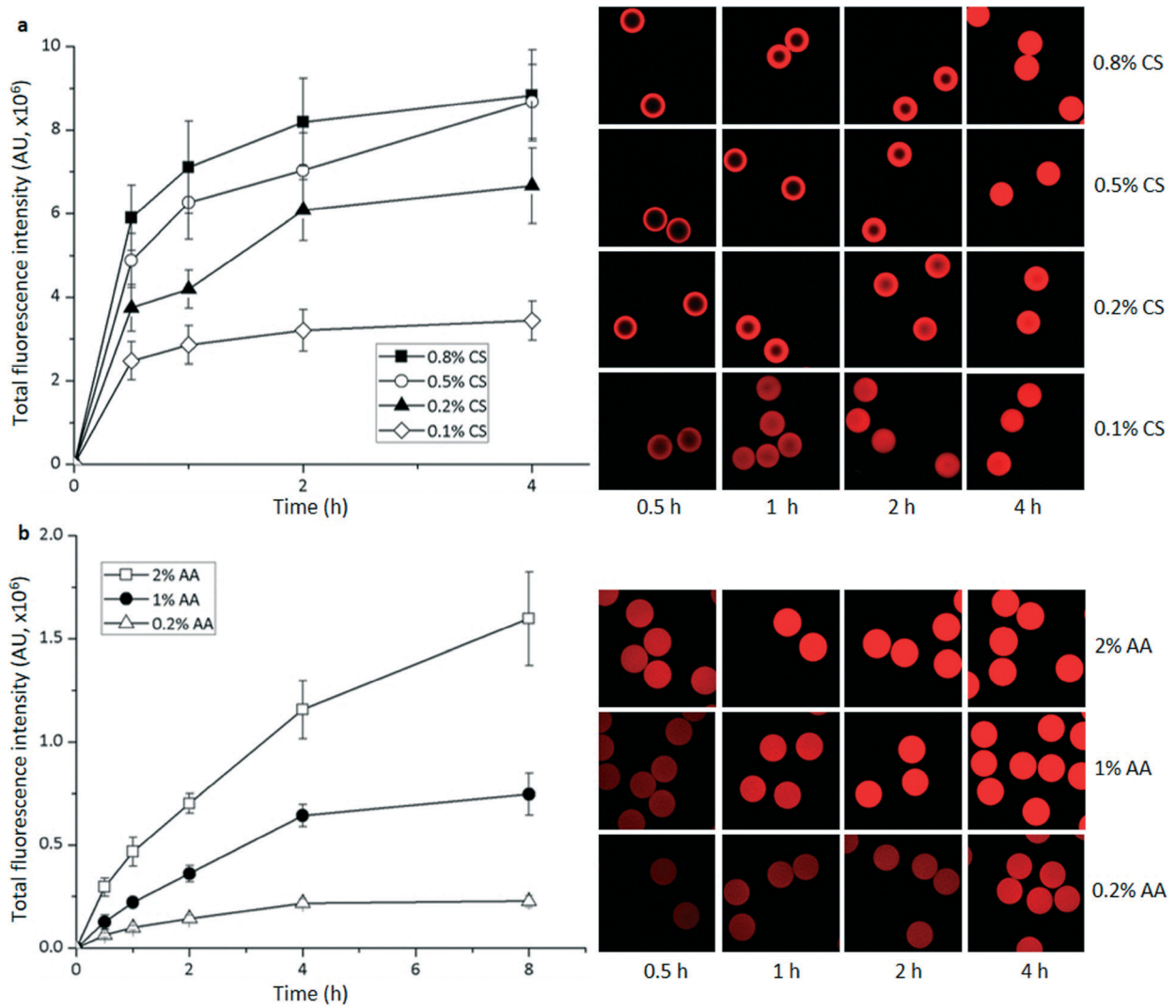

Fig. 6 Kinetic behaviour of R-PE conjugation with CS-PEG and AA-PEG microspheres. (a) Total fluorescence intensity *vs.* time plot and confocal micrographs of R-PE conjugation with CS-PEG microspheres prepared with 0.1–0.8 wt% CS. (b) Total fluorescence intensity *vs.* time plot and confocal micrographs of R-PE conjugation with AA-PEG microspheres prepared with 0.2–2 vol% AA.

Protein conjugation kinetics

Motivated by the full penetration of R-PE proteins through both types of microspheres observed in Fig. 5, we then thoroughly examined the kinetic and diffusive behaviours of CS-PEG and AA-PEG microspheres for the conjugation reactions with R-PE *via* the Tz–TCO and EDC/NHS reaction schemes respectively, as shown in Fig. 6. Specifically, Tz-activated CS-PEG and NHS ester-activated AA-PEG microspheres prepared with fixed PEGDA content and varying functional group contents were conjugated with fixed concentration of TCO-modified R-PE and R-PE respectively for up to 4 h, with measurements taken at multiple time points. Total fluorescence intensities from the resulting epifluorescence micrographs (ESI,† Fig. S1) were measured at each time point, and confocal micrographs were also taken to examine the penetration depths of R-PE through the microspheres' hydrogel networks over time.

First, as shown in the total fluorescence intensity *vs.* time plot of Fig. 6a, the fluorescence intensities of CS-PEG microspheres prepared with 0.1–0.8 wt% CS rise rapidly, reaching 60–70% of their respective maximum fluorescence intensities by 0.5 h. This rapid increase in fluorescence is most likely due to the high reaction rate of the Tz–TCO reaction (820 M^{-1} s^{-1}),[32] resulting in rapid coupling of TCO-modified R-PE with the Tz groups within the CS-PEG microspheres. In turn, the rapid reaction rate of the Tz–TCO reaction enables TCO-modified R-PE to react with Tz sites even at very low concentration, making it possible to examine diffusion while neglecting the effect of reaction rate (*i.e.*, low Damköhler number).[36] As expected, CS-PEG microspheres prepared with higher CS content yielded higher initial rates of reaction and maximum fluorescence intensities, due to the higher number of functional groups (*i.e.* Tz-activated CS) in the microspheres. In addition, the fluorescence intensities of the 0.2, 0.5, and 0.8% CS conditions continued to rise, only plateauing at 4 h, while the fluorescence intensity of the 0.1% CS condition plateaued by 1 h. This suggests that the Tz sites available within the microspheres prepared with higher CS content were consumed by TCO-modified R-PE during the 2–4 h period, while most of the Tz active sites in the 0.1% CS-PEG microspheres seem to have been consumed by 1 h. Given the rapid rate of the Tz–TCO reaction, this observed "apparent" kinetic behaviour suggests that TCO-modified R-PEs are still diffusing into the centres of the microspheres from 2–4 h for the 0.2–0.8% CS conditions, while the TCO-modified R-PEs have diffused throughout the microspheres in the 0.1% CS condition by 1 h.

This differing kinetic behaviour observed *via* epifluorescence imaging is further confirmed by confocal micrographs on the right side of Fig. 6a. Specifically, the confocal micrographs taken at the centres of CS-PEG microspheres prepared with 0.1–0.8% CS upon 0.5 h reaction show conjugation of R-PE only near the outer regions for all the four types of microspheres (first column). The centres of the microspheres prepared with 0.1% CS display bright fluorescence by 1 h and attain brighter, uniform fluorescence throughout each microsphere by 2 h (bottom row), while centres of microspheres prepared with higher CS content take increasingly longer time to display fluorescence. This indicates that R-PE can fully penetrate to the centres of microspheres prepared with 0.1% CS by 1–2 h. In contrast, the microspheres prepared with 0.2–0.8% CS show incomplete R-PE penetration into their centres at 1 h (second column), with the 0.2% CS case displaying deeper penetration than the 0.5% or 0.8% CS cases. At 2 h, the 0.2–0.8% conditions all show deeper R-PE penetration to the centres of the microspheres while maintaining a similar trend of 0.2% CS spheres displaying further penetration than 0.5% and 0.8% spheres (third column). Finally, by 4 h, all CS conditions display bright and uniform fluorescence throughout the microspheres, indicating full penetration of R-PE to the centres of the microspheres. The slower penetration of R-PE into the microspheres with higher CS content is likely due to a few factors. First, microspheres prepared with higher CS content have smaller mesh size, as observed in our recent reports.[18] Specifically, more CS molecules in the prepolymer solution should lead to higher incorporation of CS molecules as crosslinkers in the polymer networks *via* inefficient Michael addition reaction[25] and hence smaller polymer mesh size. Second, microspheres prepared with higher CS content have more active sites, allowing for more R-PEs to covalently bind to the outer regions first and sterically hinder the diffusion of subsequent R-PEs toward the centres of the microspheres. In essence, the kinetic behaviours observed in Fig. 6a is governed by the diffusion limitation of the R-PE within the polymer networks of the CS-PEG microspheres. These results indicate that CS-PEG microspheres prepared with higher CS content display higher protein binding capacity and react more rapidly, yet have smaller mesh size than the microspheres prepared with lower CS content.

Next, as shown in Fig. 6b, R-PE conjugation with AA-PEG microspheres *via* EDC/NHS chemistry displays different kinetic and diffusive behaviours than CS-PEG microspheres. First, Fig. 6b shows that the fluorescence intensities of AA-PEG microspheres prepared with 0.2–2% AA increase slowly with higher initial rates of reaction for the higher AA content conditions. Specifically, the fluorescence intensities reach 30–40% of maximum by 1 h for 0.2–2% AA conditions and plateau by 8 h. This is in direct contrast to the CS-PEG microspheres in Fig. 6a, which reach 70–80% of maximum fluorescence by 1 h and plateau by 4 h. Furthermore, the AA-PEG microspheres displayed 5–10-fold lower maximum fluorescence intensities compared to the CS-PEG microspheres. These results are likely due to the slower reaction rate of the acyl substitution reaction in contrast to the Tz–TCO reaction, along with competing hydrolysis and side reactions with the NHS ester groups in the AA-PEG microspheres consuming some of the active sites.[27,29]

The diffusive behaviour of R-PE through the AA-PEG microspheres is also different from that of the CS-PEG microspheres, as further illustrated by the confocal micrographs to the right of Fig. 6b. By 0.5 h, the centres of the microspheres

prepared with 0.2–2% AA display uniform fluorescence, indicating that R-PEs have already diffused through the polymer networks that are more macroporous than the CS-PEG microspheres (first column). The fluorescence of each type of AA-PEG microspheres continue to increase uniformly throughout each microsphere over time (second and fourth columns), again in contrast to the CS-PEG microspheres. These results thus indicate that the R-PE conjugation with NHS ester-activated AA-PEG microspheres is more reaction-controlled than the CS-PEG cases. We attribute this to larger AA-PEG microsphere mesh size arising from the poor polymerization efficiency of AA and potential charge repulsion of the negatively charged carboxylates within the microspheres,[37,38] in addition to the slower and competing nature of the NHS ester–amine reaction.

In conclusion, the results in Fig. 6 highlight the differences in kinetic and diffusive behaviour of protein conjugation with diffusion governing the CS-PEG case and both diffusion and reaction governing the AA-PEG case.

Simultaneous one-pot protein conjugation

Finally, we demonstrate orthogonal one-pot conjugation of two model fluorescent proteins R-PE and GFPuv with CS-PEG and AA-PEG microspheres *via* the Tz–TCO and EDC/NHS chemistries and simple size-based encoding as shown in Fig. 7. For this, we placed both 140 μm diameter CS-PEG microspheres and 200 μm diameter AA-PEG microspheres in one pot and added Tz-PEG_5-NHS ester (reactive only to the primary amines in the CS-PEG microspheres), as shown in the schematic diagram of Fig. 7a. Upon washing excess Tz-PEG_5-NHS ester, we then added EDC/NHS to the solution, which should react only with the carboxylates in the AA-PEG microspheres. Upon washing away excess EDC/NHS, we then simultaneously added both GFPuv and TCO-modified R-PE of varying concentrations to the microsphere solution for 1 and 4 h for the covalent coupling of TCO-modified R-PE with the CS-PEG microspheres and GFPuv with the AA-PEG microspheres respectively.

First, the brightfield micrographs in the first column of Fig. 7b show that the smaller CS-PEG and larger AA-PEG microspheres conjugated with 50 or 100 nM TCO-modified R-PE and 4 μM GFPuv are uniform and readily distinguishable, illustrating simple size-based encoding. Next, the brightfield-confocal overlays in the second column of Fig. 7b indicate the orthogonal conjugation of TCO-modified R-PE with the CS-PEG microspheres and GFPuv with the AA-PEG microspheres. Meanwhile, the negative controls (ESI,† Fig. S2) show minimal cross-talk, providing further evidence of the orthogonal nature of the two reactions.

Finally, as shown in the confocal micrographs of the centres of the microspheres in the third column of Fig. 7b, CS-PEG microspheres conjugated with higher TCO-modified R-PE content and longer time display increasing fluorescence and R-PE penetration depth. Specifically, the CS-PEG microspheres for the 50 nM R-PE case (first row) show brighter

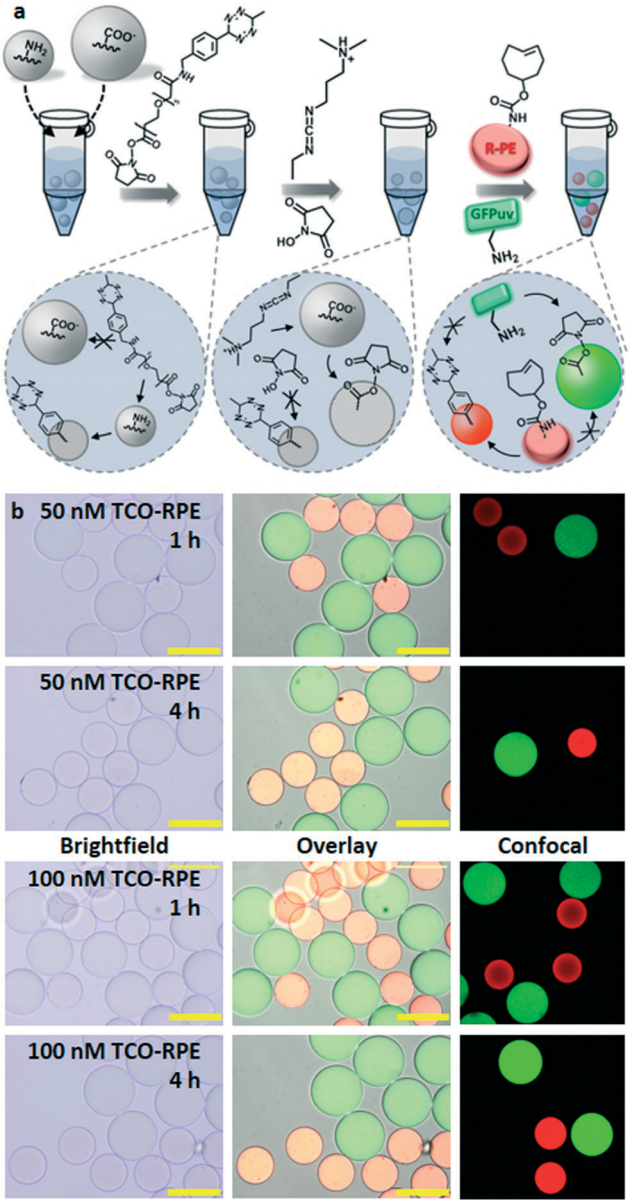

Fig. 7 One-pot conjugation of TCO-modified R-PE and GFPuv with CS-PEG and AA-PEG microspheres respectively. (a) Schematic diagram of one-pot conjugation. (b) Brightfield and confocal micrographs of 1 and 4 h one-pot conjugation of 50 or 100 nM TCO-modified R-PE and 4 μM GFPuv. Scale bars represent 200 μm.

fluorescence on the outer regions than the centres upon 1 h reaction, while AA-PEG microspheres display uniform fluorescence throughout at 1 h. At 4 h, both the CS-PEG and AA-PEG microspheres display brighter and completely uniform fluorescence, indicating complete diffusion of R-PE in CS-PEG microspheres and more proteins conjugated within both types of microspheres. This trend is also observed in the CS-PEG and AA-PEG microspheres for the 100 nM R-PE condition (third and fourth row), with CS-PEG microspheres showing incomplete R-PE penetration at 1 h and both types of microspheres displaying brighter fluorescence and complete penetration of proteins by 4 h. As expected, at 1 h reaction

the higher 100 nM concentration of R-PE leads to the brighter red fluorescence observed in CS-PEG microspheres compared to the 50 nM case above. These results indicate the orthogonal nature of the two reactions that enables simple one-pot conjugation of two different proteins with respective hydrogel microspheres.

Experimental

Hydrogen chloride, sodium hydroxide, Tween 20, 1-ethyl-3-(3-(dimethylamino)propyl)carbodiimide HCl (EDC), *N*-hydroxysuccinimide (NHS), 2-(4-morpholino)ethanesulfonic acid (MES), borate buffered saline (BBS) (20× concentrate, 50 mM borate, pH 8.5), sodium phosphate monobasic anhydrous (99%), sodium phosphate dibasic anhydrous (99%), Luria-Bertani (LB) media, ampicillin, isopropyl β-D-1-thiogalactopyranoside (IPTG), and Bradford assay kits were purchased from Thermo Fisher Scientific (Waltham, MA). Bugbuster reagent and centrifugal filter units (Amicon Ultra 0.5 mL) were purchased from EMD Millipore (Billerica, MA). Hexadecane, poly(ethylene glycol) (PEG, Mn 600 Da), poly(ethylene glycol) diacrylate (PEGDA, Mn 700 Da), chitosan oligosaccharide lactate (average Mn 5 kDa, >90% deacetylation), 2-hydroxy-2-methyl-propiophenone, acrylic acid, poly(vinyl alcohol) (87–89% hydrolyzed), *n*-octadecyltrimethoxyl silane, saline sodium citrate buffer (SSC) (20× concentrate, pH 7.0), and phosphate buffered saline (10 mM phosphate, 2.7 mM potassium chloride, 137 mM sodium chloride) pH 7.4 were purchased from Sigma-Aldrich (St. Louis, MO). 5- (and 6-) carboxyfluorescein succinimidyl ester (NHS-fluorescein) was purchased from Pierce Biotechnology (Rockford, IL). Dimethyl sulfoxide was purchased from ACROS Organics (Geel, Belgium). R-Phycoerythrin (R-PE) was purchased from Anaspec Incorporated (Fremont, CA). *trans*-Cyclooctene-poly(ethylene glycol)-*N*-hydroxysuccinimide ester (TCO-PEG_4-NHS ester) and tetrazine-PEG_5-NHS ester were purchased from Click Chemistry Tools (Scottsdale, AZ). Fluoresceinyl glycine amide (FGA) was purchased from Setareh Biotech (Eugene, OR). Imidazole was purchased from Amresco (Solon, OH). ABIL EM 90 was purchased from Evonik Industries (Germany). 2-[Methoxy(polyethyleneoxy)propyl]trimethoxy silane was purchased from Gelest (Morrisville, PA). The glass capillaries were purchased from AIT Glass (Rockaway, NJ). All chemicals were analytical grade and used without further purification.

Fabrication of capillary microfluidic device and drop generation

We first prepared injection capillaries by tapering circular glass capillaries (1B100-6, World Precision Instruments, Inc., Sarasota, FL) with 560 μm inner diameter to 50 μm inner diameter using a micropipette puller (P-97, Sutter Instrument, Novato, CA). To render surface hydrophobicity, the inner walls of the injection capillaries were treated with *n*-octadecyltrimethoxyl silane for 30 min and subsequently washed with ethanol. The circular injection capillary was then carefully inserted into the square capillary whose inner width (1.05 mm) is slightly larger than that of the outer diameter of the injection capillary (1 mm). Next, the small tapered glass capillary with 10 μm inner diameter was prepared by heating and pulling a cylindrical capillary by hand using a gas torch; this capillary was then inserted into the injection capillary for simultaneous injection of two immiscible fluids. Finally, the circular collection capillary was inserted into the square capillary from the other end; we also treated this collection capillary with 2-[methoxy(polyethyleneoxy)propyl]-trimethoxy silane to make the capillary wall hydrophilic. During drop generation, the volumetric flow rate was controlled by syringe pumps (Harvard Apparatus, Holliston, MA) and the production of the emulsion drops was observed using an inverted microscope equipped with a high-speed camera (Vision Research Inc., Phantom V9.0, Wayne, NJ).

Fluorescent labelling with CS-PEG microspheres

As-prepared CS-PEG microspheres were reacted with 100 μM NHS-fluorescein in 5× saline sodium citrate (SSC) buffer containing 0.05 vol% Tween 20 (SSC-TW20 buffer solution) (pH 7) or 20 mM sodium phosphate buffer (SPB) containing 0.05 vol% Tween 20 (SPB-TW20) (pH 6, 7, 8, or 9) for 1 h, then washed with DI water (1×), DMSO (2×), and SSC-TW20 buffer (pH 7) (3×) to remove excess unreacted and non-specifically bound NHS-fluorescein.

Protein modification with TCO

To prepare TCO-modified R-PEs, we first exchanged the buffer solution of the R-PE with BBS (50 mM borate, 300 mM sodium chloride, pH 8.5) *via* centrifugal filtration units at 4 °C. The R-PEs were then reacted with 20- or 50-fold molar excess TCO-PEG_4-NHS ester for 30 min at room temperature and then purified from the unreacted excess TCO molecules *via* centrifugal filtration with phosphate buffered saline pH 7.4. The final concentrations of the purified TCO-modified R-PE were measured using UV-visible spectroscopy (Evolution 300 UV-vis spectrophotometer, Thermo Scientific) with the characteristic absorbance peak (565 nm) and molar extinction coefficient (1.96×10^6 M^{-1} cm^{-1}) of the R-PE.[39]

R-PE conjugation with CS-PEG microspheres

R-PE conjugation with CS-PEG microspheres was performed using tetrazine–*trans*-cyclooctene chemistry.[31] First, CS-PEG microspheres were activated with 500 μM tetrazine-PEG_5-NHS ester for 1 h in SSC-TW20 buffer (pH 7) at room temperature. The Tz-activated CS-PEG microspheres were washed with SSC-TW20 buffer (pH 7) (5×) and then reacted with 50 nM to 2 μM TCO-modified R-PE for up to 8 h in SSC-TW20 buffer (pH 7) at room temperature, with samples collected at various time points. The microspheres were then washed with SSC-TW20 buffer (pH 7) (5–6×).

Fluorescent labelling with AA-PEG microspheres

To label the AA-PEG microspheres with FGA, we first activated the AA-PEG microspheres with 0.4 M EDC and 0.1 M

NHS in 20 mM MES buffer containing 0.05 vol% Tween 20 (MES-TW20) (pH 6) for 15 min to provide a high number of NHS ester functional groups as indicated in our recent report,[18] and then washed away the unreacted excess with MES-TW20 buffer (pH 6) (2×) and SPB-TW20 buffer (pH 6, 7, 8, or 9) (2×). Upon reaction with FGA in SPB (pH 6, 7, 8, or 9) for 1 h, the microspheres were then washed with DI water (1×), DMSO (2×) and SSC-TW20 buffer (pH 7) (3×) to remove excess unreacted and non-specifically bound FGA.

Production and purification of green fluorescent proteins (GFPuv)

Green fluorescent protein modified for maximum fluorescence under UV light (GFPuv) was generously provided by Dr. Chen-Yu Tsao and Dr. William E. Bentley at University of Maryland in *E. coli* BL 21 harbouring the plasmid ptrcHisB::gfpuv,[40] and obtained *via* standard protein expression methods. Briefly, the *E. coli* cells were cultivated in LB media in flask cultures, and the GFPuv expression was induced by adding 0.4 mM IPTG. Upon harvesting and disrupting the cells with Bugbuster, a standard 1 mL immobilized metal affinity chromatography (IMAC) column (GE Healthcare, Chicago, IL) was utilized to purify the hexahistidine-tagged GFPuv using 0.5 M imidazole as the displacer. The as-prepared GFPuv was quantified by a standard Bradford assay[41] and used in the protein conjugation studies without further purification.

R-PE conjugation with AA-PEG microspheres

To conjugate R-PE with the AA-PEG microspheres, we first activated the microspheres with 0.4 M EDC and 0.1 M NHS in MES-TW20 buffer (pH 6) for 15 min. Upon washing with MES-TW20 buffer (pH 6) (2×) and SSC-TW20 buffer (pH 8) (2×), we then reacted the NHS ester-activated AA-PEG microspheres with 2 μM R-PE for up to 8 h in SSC-TW20 buffer (pH 8) at room temperature, taking sample measurements at various time points. The microspheres were then washed with SSC-TW20 buffer (pH 7) (5–6×).

One-pot GFPuv and TCO-modified R-PE conjugation with CS-PEG and AA-PEG microspheres

CS-PEG (140 μm diameter) and AA-PEG (200 μm diameter) microspheres were placed together in SSC-TW20 buffer (pH 7). We then activated the spheres with 500 μM Tz for 1 h at room temperature. Upon washing away excess unreacted Tz with SSC-TW20 buffer (pH 7) (2×) and MES-TW20 buffer (pH 6) (2×), we then activated the spheres with 0.4 M EDC and 0.1 M NHS in MES-TW20 buffer for 15 min. We then washed away excess with SSC-TW20 buffer (pH 8) and added 4 μM GFPuv and 50–100 nM TCO-modified R-PE to the solution for 1 or 4 h. The GFPuv-conjugated AA-PEG and TCO-modified R-PE-conjugated CS-PEG microspheres were then washed with SSC-TW20 buffer (pH 7) (5–6×).

Image analysis

The fluorescently labelled and protein-conjugated microspheres were imaged with an epifluorescence microscope (Olympus BX51 equipped with a DP70 microscope digital camera, Centre Valley, PA) and a confocal microscope (Leica DMIRE2 equipped with a TCS SP2 scanner, Wetzlar, Germany), all in SSC-TW20 buffer (pH 7). Epifluorescence micrographs of these microspheres were obtained with a 10× objective lens under standard green (U-N31001), red (U-N31002), and UV (11000v3) filter sets (Chroma Technology Corp., Rockingham, VT). Confocal micrographs of the protein-conjugated microspheres were obtained with a 10× and 20× objective lens under 488 and 543 nm excitation with depth scan increments of 10–20 μm. Fluorescence intensity and microsphere diameter measurements were done using ImageJ image analysis software.[42]

Conclusions

In this work, we presented a reliable and rapid one-step microfluidic approach utilizing double emulsion drops with an ultra-thin sacrificial oil shell to fabricate highly monodisperse hydrogel microspheres with tunable size and chemical functionality in a simple, consistent and cost-efficient manner. Simple fluorescent labelling studies demonstrated the abundant and uniformly distributed primary amines (CS-PEG) or carboxylates (AA-PEG), with the primary amines of CS representing an efficient conjugation handle at neutral pH. The utility of these microspheres for biomolecular conjugation was demonstrated using large fluorescent protein R-PE *via* Tz–TCO and EDC/NHS schemes, where confocal microscopy illustrated that diffusion primarily governs the protein conjugation of CS-PEG microspheres with smaller mesh size, while diffusion and reaction both govern the protein conjugation of AA-PEG microspheres with larger mesh size. Finally, the one-pot protein conjugation results showed orthogonality and simple size-based encoding afforded by our integrated approach combining potent capillary microfluidic fabrication and selective bioconjugation. These results represent a significant advancement in the rapid and tunable fabrication of hydrogel microspheres with precise control over size and chemical functionality over previous works, as well as their potential for biomolecular applications through the rapid and selective conjugation of large proteins.

While not examined in this report, our fabrication–conjugation approaches are highly modular and can be readily extended to impart numerous other features. On the fabrication side, the choice of a range of monomers and multiple functional groups can impart additional functionality onto the microspheres, such as *N*-isopropylacrylamide for thermal responsiveness,[43] higher acrylic acid content for pH-based responsiveness,[44] or caprolactone for biodegradability,[45] to name a few. These functions could also be further enhanced through the inclusion of multiple compartments within the microspheres for isolation of functions and other features.[17,46] On the conjugation side, conjugation of various

molecules of interest such as antibodies[47] or peptide probes[48] with our chemically functional microspheres can enable the capture of biospecific targets toward rapid biosensing or medical diagnostic applications. The chemically functional microspheres can also take advantage of a suite of click chemistries[49] for the rapid and orthogonal conjugation of multiple probes or molecules of interest. We thus envision that our integrated fabrication–conjugation approach could be readily adopted to manufacture hydrogel microparticles with multifaceted dimensional, functional and specific features for a wide range of applications.

Conflicts of interest

There are no conflicts to declare.

Acknowledgements

We gratefully acknowledge partial financial support by the National Research Foundation of Korea (NRF) grant funded by the Korea government (NRF-2017R1C1B2006237), the U.S. National Science Foundation (Grant # CBET-1703549), the National Science Foundation (DMR-1708729), and the Harvard Materials Research Science and Engineering Center (NSF DMR-1420570), and the National Institutes of Health (R01EB014703).

References

1 G. C. Le Goff, R. L. Srinivas, W. A. Hill and P. S. Doyle, *Eur. Polym. J.*, 2015, **72**, 386–412.
2 X. Xie, W. Zhang, A. Abbaspourrad, J. Ahn, A. Bader, S. Bose, A. Vegas, J. Lin, J. Tao, T. Hang, H. Lee, N. Iverson, G. Bisker, L. Li, M. S. Strano, D. A. Weitz and D. G. Anderson, *Nano Lett.*, 2017, **17**, 2015–2020.
3 K. Chen, T. J. Merkel, A. Pandya, M. E. Napier, J. C. Luft, W. Daniel, S. Sheiko and J. M. DeSimone, *Biomacromolecules*, 2012, **13**, 2748–2759.
4 A. Z. M. Badruddoza, P. D. Godfrin, A. S. Myerson, B. L. Trout and P. S. Doyle, *Adv. Healthcare Mater.*, 2016, **5**, 1960–1968.
5 A. Khademhosseini and R. Langer, *Biomaterials*, 2007, **28**, 5087–5092.
6 X. Zhao, S. Liu, L. Yildirimer, H. Zhao, R. Ding, H. Wang, W. Cui and D. Weitz, *Adv. Funct. Mater.*, 2016, **26**, 2809–2819.
7 N. A. Peppas, J. Z. Hilt, A. Khademhosseini and R. Langer, *Adv. Mater.*, 2006, **18**, 1345–1360.
8 M. T. Gokmen and F. E. Du Prez, *Prog. Polym. Sci.*, 2012, **37**, 365–405.
9 Y. Du, E. Lo, S. Ali and A. Khademhosseini, *Proc. Natl. Acad. Sci. USA*, 2008, **105**, 9522–9527.
10 C. J. Hernandez and T. G. Mason, *J. Phys. Chem. C*, 2007, **111**, 4477–4480.
11 C.-H. Choi, J. Kim, S.-M. Kang, J. Lee and C.-S. Lee, *Langmuir*, 2013, **29**, 8447–8451.
12 S. Jung, J. H. Abel, J. L. Starger and H. Yi, *Biomacromolecules*, 2016, **17**, 2427–2436.
13 S. Jung, C.-H. Choi, C.-S. Lee and H. Yi, *Biotechnol. J.*, 2016, **11**, 1561–1571.
14 J. H. Kim, T. Y. Jeon, T. M. Choi, T. S. Shim, S.-H. Kim and S.-M. Yang, *Langmuir*, 2014, **30**, 1473–1488.
15 H. Lee, S. J. Shapiro, S. C. Chapin and P. S. Doyle, *Anal. Chem.*, 2016, **88**, 3075–3081.
16 C.-H. Choi, H. Wang, H. Lee, J. H. Kim, L. Zhang, A. Mao, D. J. Mooney and D. A. Weitz, *Lab Chip*, 2016, **16**, 1549–1555.
17 S.-H. Kim, J. W. Shim and S.-M. Yang, *Angew. Chem., Int. Ed.*, 2011, **50**, 968–968.
18 E. Y. Liu, S. Jung and H. Yi, *Langmuir*, 2016, **32**, 11043–11054.
19 H. Yi, L.-Q. Wu, W. E. Bentley, R. Ghodssi, G. W. Rubloff, J. N. Culver and G. F. Payne, *Biomacromolecules*, 2005, **6**, 2881–2894.
20 S.-H. Kim, J. W. Kim, J.-C. Cho and D. A. Weitz, *Lab Chip*, 2011, **11**, 3162–3166.
21 C.-H. Choi, J.-H. Jung, T.-S. Hwang and C.-S. Lee, *Macromol. Res.*, 2009, **17**, 163–167.
22 D. K. Hwang, D. Dendukuri and P. S. Doyle, *Lab Chip*, 2008, **8**, 1640–1647.
23 S.-H. Kim and D. A. Weitz, *Angew. Chem., Int. Ed.*, 2011, **50**, 8731–8734.
24 S. Jung and H. Yi, *Chem. Mater.*, 2015, **27**, 3988–3998.
25 B. D. Mather, K. Viswanathan, K. M. Miller and T. E. Long, *Prog. Polym. Sci.*, 2006, **31**, 487–531.
26 S. Jung and H. Yi, *Langmuir*, 2012, **28**, 17061–17070.
27 J. V. Staros, R. W. Wright and D. M. Swingle, *Anal. Biochem.*, 1986, **156**, 220–222.
28 K. D. Schwenke, in *Food Proteins: Properties and Characterization*, ed. S. Nakai and H. W. Modler, WILEY-VCH Verlag GmbH, New York, 1996, ch. 2, vol. 40, pp. 22–35.
29 S. Sam, L. Touahir, J. Salvador Andresa, P. Allongue, J. N. Chazalviel, A. C. Gouget-Laemmel, C. Henry de Villeneuve, A. Moraillon, F. Ozanam, N. Gabouze and S. Djebbar, *Langmuir*, 2010, **26**, 809–814.
30 G. R. Grimsley, J. M. Scholtz and C. N. Pace, *Protein Sci.*, 2009, **18**, 247–251.
31 M. L. Blackman, M. Royzen and J. M. Fox, *J. Am. Chem. Soc.*, 2008, **130**, 13518–13519.
32 M. R. Karver, R. Weissleder and S. A. Hilderbrand, *Bioconjugate Chem.*, 2011, **22**, 2263–2270.
33 M. Goulian and S. M. Simon, *Biophys. J.*, 2000, **79**, 2188–2198.
34 R. Langer and D. A. Tirrell, *Nature*, 2004, **428**, 487–492.
35 N. A. Peppas and S. L. Wright, *Macromolecules*, 1996, **29**, 8798–8804.
36 D. C. Pregibon and P. S. Doyle, *Anal. Chem.*, 2009, **81**, 4873–4881.
37 K. S. Anseth, R. A. Scott and N. A. Peppas, *Macromolecules*, 1996, **29**, 8308–8312.
38 J. E. Elliott, M. Macdonald, J. Nie and C. N. Bowman, *Polymer*, 2004, **45**, 1503–1510.
39 M.-H. Yu, A. N. Glazer, K. G. Spencer and J. A. West, *Plant Physiol.*, 1981, **68**, 482–488.
40 C.-F. Wu, H. J. Cha, G. Rao, J. J. Valdes and W. E. Bentley, *Appl. Microbiol. Biotechnol.*, 2000, **54**, 78–83.

41 M. M. Bradford, *Anal. Biochem.*, 1976, **72**, 248–254.
42 C. A. Schneider, W. S. Rasband and K. W. Eliceiri, *Nat. Methods*, 2012, **9**, 671–675.
43 T. Hoare and R. Pelton, *Macromolecules*, 2004, **37**, 2544–2550.
44 G. R. Mahdavinia, A. Pourjavadi, H. Hosseinzadeh and M. J. Zohuriaan, *Eur. Polym. J.*, 2004, **40**, 1399–1407.
45 C. H. Yang, K. S. Huang, Y. S. Lin, K. Lu, C. C. Tzeng, E. C. Wang, C. H. Lin, W. Y. Hsu and J. Y. Chang, *Lab Chip*, 2009, **9**, 961–965.
46 X. Yu, G. Cheng, M.-D. Zhou and S.-Y. Zheng, *Langmuir*, 2015, **31**, 3982–3992.
47 B. Guan, A. Magenau, S. Ciampi, K. Gaus, P. J. Reece and J. J. Gooding, *Bioconjugate Chem.*, 2014, **25**, 1282–1289.
48 E. Aoraha, J. Candreva and J. R. Kim, *Mol. BioSyst.*, 2015, **11**, 2281–2289.
49 C. S. McKay and M. G. Finn, *Chem. Biol.*, 2014, **21**, 1075–1101.